Velocity Measurement during Evaporation of Seeded, Sessile Drops on Heated Surfaces

John R.E. CHRISTY [*1], Khellil SEFIANE [1], Benoit ROMAIN [1]

* Corresponding author: Tel.: ++44 (0)131 6504854; Fax: ++44 (0)131 6506551; Email: J.Christy@ed.ac.uk
1. School of Engineering, University of Edinburgh, UK

Abstract Evaporation of sessile drops has been studied extensively in an attempt to understand the effect of wetting on the evaporation process. Recently interest has also increased in the deposition of particles from such drops, with evaporative mass flux being deemed to be responsible for ring-like deposits and Marangoni convection counteracting this mass flux explaining more uniform deposition patterns. Understanding of such deposition processes is important in ink-jet printing and other micro-scale deposition technologies, where the nature of deposition can have a dramatic effect on the quality or effectiveness of the finished product. In most cases where deposition from evaporating drops has been studied, velocity information is inferred from the final deposition pattern or from mathematical modeling based on simplified models of the physics of the evaporation process. In this study we have directly measured the flow velocities in the base of sessile drops, using micro-PIV, viewing the drop from below, through the cover slide. The images obtained have also enabled us to observe the formation of holes in the liquid film during the latter stages of evaporation.

Keywords: Evaporation, sessile drop, velocimetry, particle deposition, μPIV

1. Introduction

The evaporation of a sessile water droplet on glass surface was studied by Birdi et al (1989), measuring the change of weight of droplets. They concluded that for most of the time during the evaporation the evaporation rate remains constant.
Further experimental studies of evaporating sessile drops, by Bourges-Mounnier et al (1995), Anderson (1995) and others have revealed at least three distinct stages of evaporation:

- Stage I: the surrounding atmosphere becomes saturated in the vapour of the evaporating liquid, with the contact angle practically constant.
- Stage II: the droplet base width remains constant as the contact angle and droplet height decrease. The contact line is effectively pinned during this stage.
- Stage III: the contact angle remains constant as the droplet base and the height decrease. The onset of this stage is due to depinning of the contact line, with this stage representing recession of the contact line. For water on glass surfaces, the contact angle below which recession takes place is reported as being about 2–4° (Hu et al 2001).

A fourth stage, that of final evaporation of the droplet, has been difficult to study due to the small drop dimensions.
Stages II and III are represented schematically in Fig. 1.

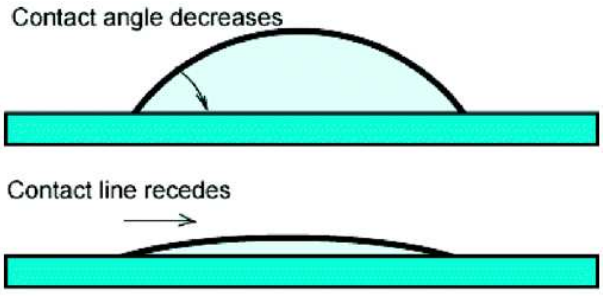

Fig. 1. A schematic of the droplet-evaporation process (Hu et al 2005a)

The presence of particles in the evaporating fluid has been found to extend stage II of the evaporation process, since deposition of

particles at the contact line aids the pinning process. Deegan et al (1997, 2000) examining the phenomenon of ring formation during drying of a drop, suggest that the formation of the ring results from pinning of the contact line and evaporation from the droplet driving fluid towards the contact line. The competition between this 'self-pinning' and 'de-pinning' can give rise to pattern formation of droplet deposits (Shmuylovich et al 2002, Adachi et al 1995).

Deegan et al (2000) found that changing the surface material, the evaporating fluid, humidity, temperature and pressure prevent the particles depositing in a ring at the contact line. They ruled out the effect of gravity by showing that the deposition pattern is the same for both a pendant and a sessile drop. However, when the drop is not pinned, as is the case on a smooth or hydrophobic surface, the deposition is uniform. This was also found to be the case by Uno et al (1998). Deegan et al (2000) also found that eliminating preferential evaporation from the contact line led to more uniform deposition. In experiments in which the sessile drop was covered by a lid with only a small hole over the centre of the drop, deposition of particles was uniform across the base of the drop. Deegan proposed a diffusional model for vapour from the drop surface to the bulk air to explain the enhanced convection at the contact line that leads to the internal liquid flow towards the contact line.

A number of researchers (e.g. van Nguyen et al 2003, Ristenpart et al 2008, Fischer 2002) have postulated that the pattern of deposition is due to competition between flows induced by evaporative mass transfer towards the contact line and Marangoni flows induced by temperature gradients towards the centre of the drop. Some researchers have claimed that Marangoni flows are insignificant for water droplets, though Xu et al (2007) have shown that this is not the case, with the Marangoni effect modifying flow in the vicinity of the contact line. Zhang et al (2008) demonstrated that the Marangoni flow can counteract evaporative mass transfer, by adding formamide to aqueous suspensions to enhance the Marangoni flow.

Computational models, such as those proposed by Deegan (2000), Hu et al (2005a,b) and Fischer (2002) have been used to explain convective flows within evaporating droplets, often with significant simplifications of the physical model: for instance, some models ignore the Marangoni effect. These models have been modified in the light of experimental evidence. However, obtaining velocity information from within small drops is far from straightforward. Viewed from above or from the side, surface curvature distorts the image, and even when such effects are accounted for (eg Kang et al 2003) there are often regions close to the contact line that cannot be viewed. To avoid distortion, in this study we have chosen to view through the base of the drop.

In this paper we apply Micro Particle Image Velocimetry (μPIV) to elucidate the flow velocities in the base of a sessile droplet during evaporation of the drop. Particle Image Velocimetry (PIV) is a full-field velocimetry technique, involving instantaneous observation of particles in an illuminated plane within the fluid and subsequent correlation of that image with images taken after known time delays (Fig. 2.).

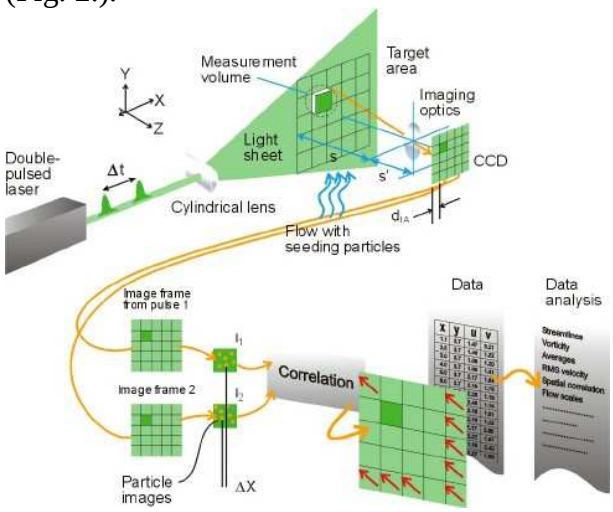

Fig. 2. Schematic diagram to illustrate the principles of PIV (Dantec Dynamics)

Micro-PIV (μPIV) is an extension of PIV to access micro-scale devices. It is an optical technique which permits detailed velocity measurements across a planar region within a fluid. Velocities are acquired by tracking the trajectories of micron-sized fluorescent seeding particles immersed in the flow. The particles are illuminated by two short pulses of laser light to obtain two digital images of the fluid separated by a known time delay, Dt. The two images produced are then divided into small interrogation areas, which are cross-correlated with each other to determine the most probable local displacement of the particles, Dx. The local velocity of the fluid v is determined by dividing the displacement by the time delay (Dx/Dt). A vector map is obtained by repeating the cross correlation for each interrogation area over the two images. This technique is inherently more accurate than streak photography techniques in that errors due to out of plane motion are eliminated.

Experimental Method

High-speed micro-PIV was used to obtain velocity information within evaporating sessile drops. For each experiment, 0.1 μl droplets of distilled water, seeded with known concentration of fluorescent micro-spheres (1μm diameter, Nile-red, carboxylate modified FluoSphere® beads of density 1.05g/cm^3) were injected onto a clean glass cover slide, sitting on an inverted microscope (Leica DM15000 M) to yield sessile drops of about 1mm diameter. The drop was covered by a 10cm x 10cm x 10cm box to guard against exposure to laser light: the humidity in the region of the drop therefore rises during the 3 to 5 minute duration of the experiment.
A New Wave Pegasus pulsed diode laser, emitting at 527nm, synchronized with a Dantec Dynamics Nanosense II camera (512x512 pixels) at 50Hz for recording images, was used to cause the particles to fluoresce at 575nm and the resulting images captured. The whole flow field is illuminated, with the thickness of the plane in which images are recorded being determined by the depth of field of the microscope (about 50μm). The image slice was positioned just above the surface, picking up layered particles on the surface along with moving particles up to 50μm from the surface. Velocities of the particles were determined by cross-correlation of successive images. In addition, particle deposition patterns were recorded following dry-out of the drop.
Prior to each experiment, the cover-slides were cleaned, rinsed in distilled water and dried using acetone. Four particle concentrations (solutions labeled ‘0’, ‘1’, ‘2’ and ‘3’ containing 0.054%, 0.027%, 0.009% and 0.0018% solids respectively) were used and the effect of particle concentration on both flow velocities within the drop and the thickness of deposit at the contact line determined. The experiments were repeated for all four concentrations on cover slides that had been heated in an oven to 10°C, 20°C and 30°C above room temperature (about 25°C).

The acquired images were analysed with Dantec Flow Manager 4.71 software by cross correlation to obtain velocity vectors plots, with vector validation based on correlation peak ratio.

Results

A sample image for a water droplet on a cover-slide at room temperature is shown in Fig. 3 and a sequence of vector maps from the same experimental run is given in Fig. 4.

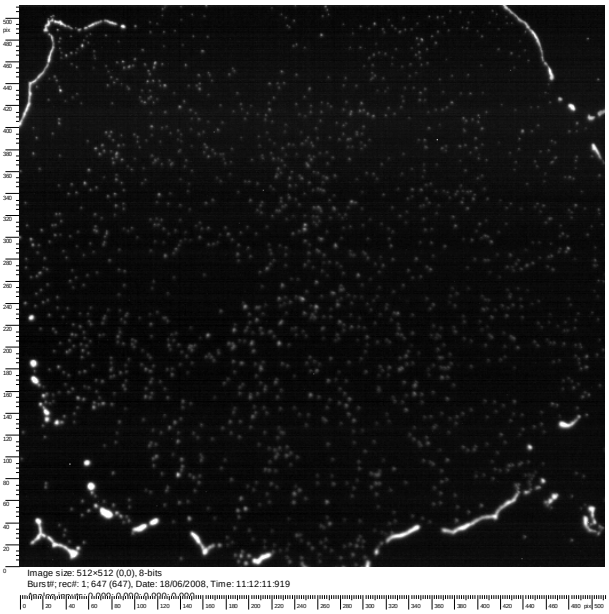

Fig. 3. Instantaneous PIV image during evaporation of a water droplet – taken towards end of run. There is evidence of some depinning in the lower left hand corner

In all experiments the particle velocities were almost always radially outwards, with the magnitude of the velocities increasing towards the contact line. For most of the droplet lifespan the contact line remains fixed, only retracting rapidly at the end as dry-out of the drop approaches. The peak velocities are about $3.5\text{x}10^{-4}$ m/s.

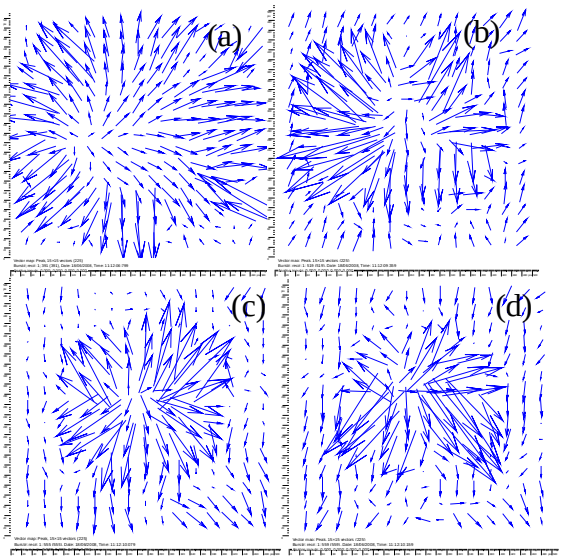

Fig. 4. sequence of vector maps for a water droplet evaporating

In these experiments the velocities are measured close to and parallel to the base of the drop. Given the magnitude of velocities relative to the relatively low evaporation rate, it is possible that the flow is enhanced by circulation currents set up by Marangoni-induced convection along the liquid gas interface. The Marangoni effect is induced by a surface tension gradient generated by a composition or temperature variation along the free liquid surface. Whilst there is debate over the sense in which Marangoni forces should act on the unheated surface (either the top of droplet should be the coolest due to its longer conduction distance from the substrate or the temperature at the edge of the droplet is colder than that at the top because the evaporation rate is larger at the edge than at the top), in the case of the heated substrate the Marangoni flow should be driven towards the apex of the drop. The expected internal flow is thus similar to that prediced by Hu et al (2005b), shown in Fig. 5.

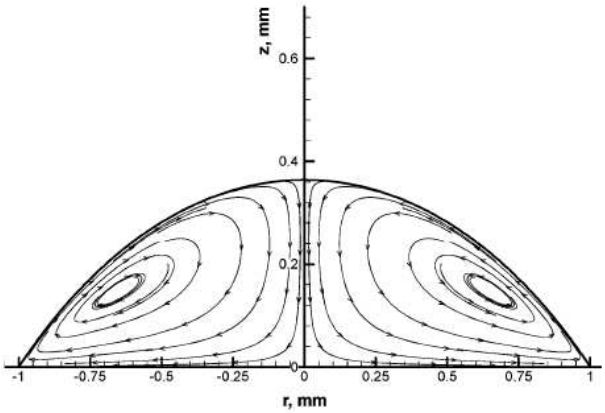

Fig. 5. streamline plots of the flow simulation (Hu et al 2005b)

The tendency for Marangoni convection to occur can be predicted from the value of the Marangoni number ($\text{Ma} = \dfrac{\dfrac{\partial \sigma}{\partial T}\Delta T\, L}{\mu \alpha}$), where ΔT is the temperature difference along the interface, L is a characteristic length, μ is the dynamic viscosity of the liquid and α is the thermal diffusivity of the liquid. We have chosen to use the difference between the substrate temperature and ambient temperature for ΔT and the radius of the base of the drop for L to be consistent with Ruiz et al (2002), rather than with values based on more sophisticated simulations (Girard et al 2008). If Ma exceeds a critical value, commonly taken to be 80, Marangoni convection is expected to take place. The values of Marangoni number in our experiments were 0, 5170, 10300 and 15500 for the unheated surface and the heated surfaces at 10°C, 20°C and 30°C above ambient respectively. Thus, for all but the unheated substrate Marangoni convection is expected in our experiments. For an unheated surface, Xu et al (2007) have shown that in spite of the expectation of zero Ma by our present estimation method, Marangoni flows can indeed exist.

If all of the evaporation occurs at the triple line and the resulting convection transports particles to this region so that they deposit almost exclusively as a ring, then the thickness of this ring should be approximately

proportional to the square root of the initial particle concentration (since it would be expected that both the height and width of the ring will increase as deposition proceeds) and independent of the cover-slide temperature. Figure 6, showing the thickness of final ring deposit against particle concentration for different Marangoni numbers, reveals that although this is largely the case, there is some variation with Marangoni number. The fact that the deposition on an unheated surface is not significantly different from that on a heated surface would suggest that, although we predict Ma = 0 for the unheated surface, any Marangoni effects found on the heated surface are also present for the unheated surface, in line with the results reported by Xu et al (2007).

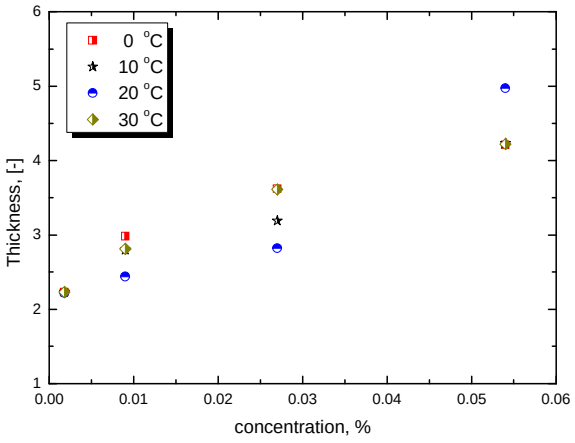

Fig. 6. thickness of the triple line deposition as a function of particle concentration

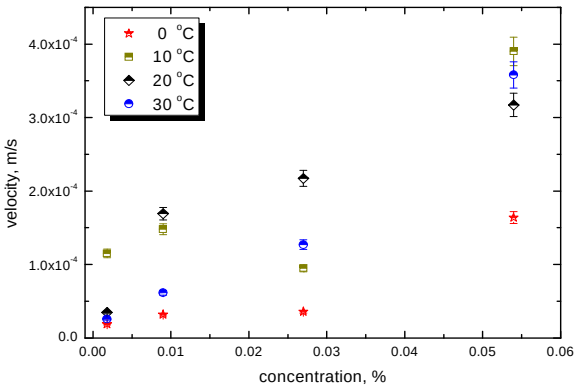

Fig. 7. average speed of the radial flow as a function of particle concentration

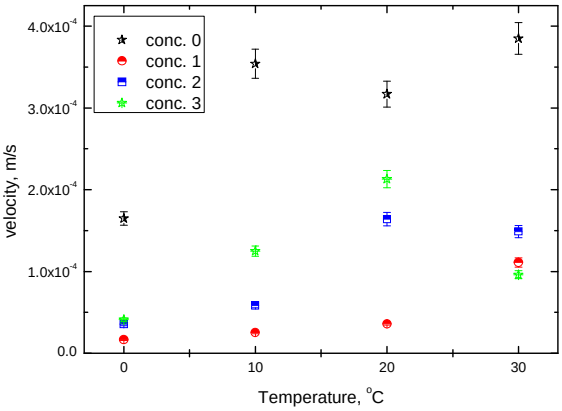

Fig. 8. spatial average speed of the radial flow as a function of substrate temperature and hence Marangoni number

For each image, a spatial average speed of the flow was calculated. This is plotted as a function of the particle concentration in Figure 7 and as a function of substrate temperature, and hence Marangoni number in Figure 8.

Surprisingly, there appears to be a stronger correlation between particle concentration and induced flow than between substrate temperature, and hence Marangoni number, and induced flow. There is still a discernable trend towards higher velocities at higher substrate temperatures. This will be linked to higher evaporation rates, as the temperature of the liquid at the contact line is close to that of the substrate, but may also be the result of Marangoni convection, which is stronger when the substrate temperature is increased relative to that of the liquid at the apex of the drop. The circulation set up will enhance the evaporation-driven flow along the base of the drop by recirculating fluid along the the air-liquid interface towards the apex of the drop.

This effect of particle concentration is both surprising and important, as previous researchers, discussing evaporation induced flow, have not commented on it. Localised velocimetry measurements rely on seeding the flow with tracer particles: if, as we have shown, the concentration of these particles influences the magnitude of the velocities

measured, then the concentration and nature of particles used must be carefully reported and consistent values used if comparisons between velocimetry data between experiments is to have any value.

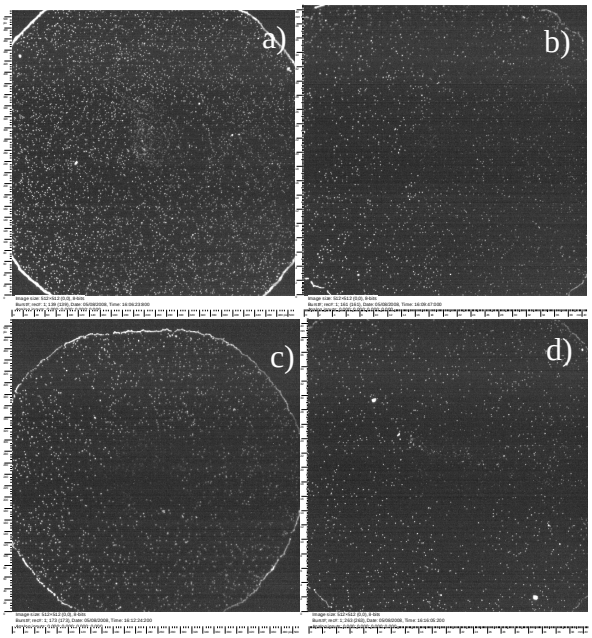

Fig. 9: cover-slides at end of evaporation period for drop at room temperature. (a) solution 0, (b) solution 1, (c) solution 2, (d) solution 3.

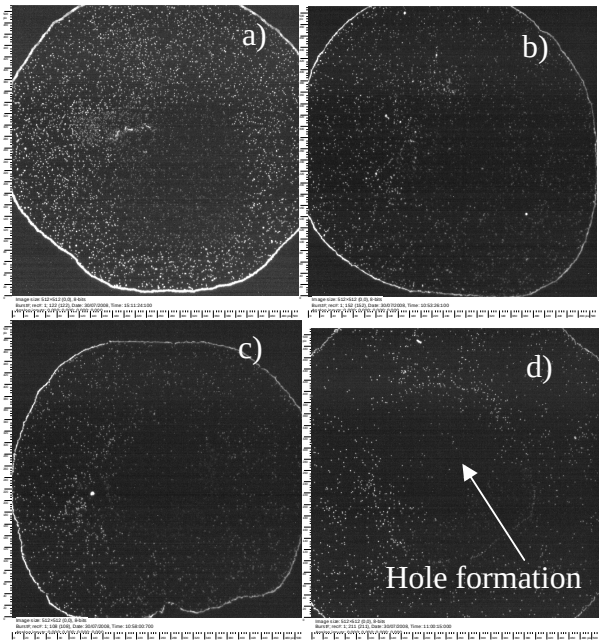

Fig. 10. cover-slides at end of evaporation period for drop at 10°C above room temperature. (a) solution 0, (b) solution 1, (c) solution 2, (d) solution 3.

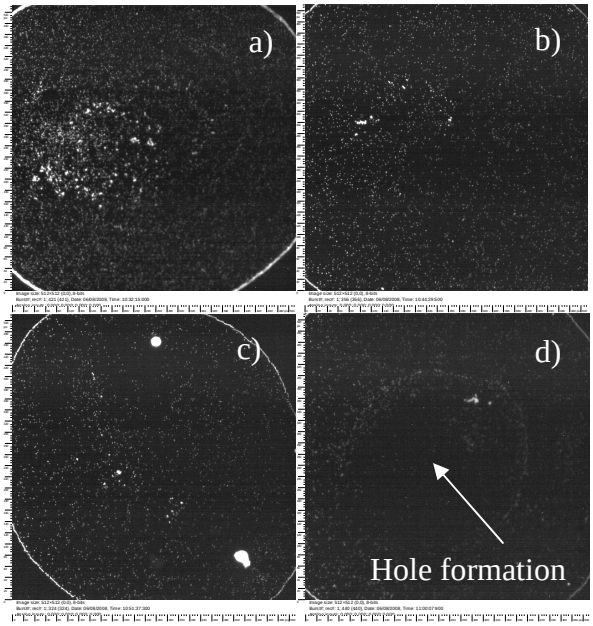

Fig. 11. cover-slides at end of evaporation period for drop at 20°C above room temperature. (a) solution 0, (b) solution 1, (c) solution 2, (d) solution 3.

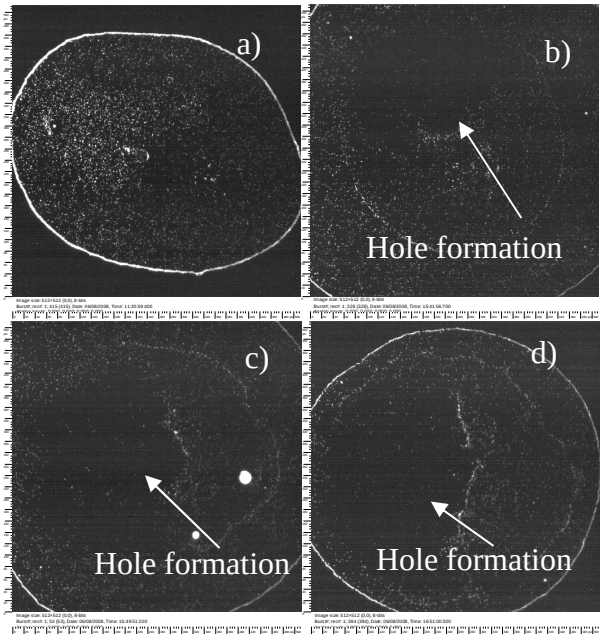

Fig. 12. cover-slides at end of evaporation period for drop at 30°C above room temperature. (a) solution 0, (b) solution 1, (c) solution 2, (d) solution 3.

The increased velocities at higher particle concentration may be due to the particles modifying the surface tension forces, and thus increasing Marangoni convection with its resultant fluid recirculation within the drop, or

to the presence of more particles at the contact line leading to greater evaporation in this region.

In figures 9 to 12, showing the latter stage of evaporation with differing concentrations of seeding particles on both unheated and heated cover-slides as dry-out is approached, we observe the development of 'holes' in which no particles have deposited for the heated cover-slides at the lower particle concentrations. The development of holes at higher concentrations appears to be related to the temperature of the cover-slide, with higher temperature increasing the concentration at which holes can appear.

Concerning the formation of holes in the latter stages of evaporation, when the drop approximates to a thin film over the substrate, they appear to differ from those observed by Deegan (2000a), in that they only appear in the final stages of evaporation and they originate in the central region of the drop, rather than next to the pinned contact line.

Ohara et al (1997) have studied the evaporation of droplets containing nano-sized particles (3-5 nm in diameter whereas our particles have a diameter of 1 μm). They observed that the particles are so small that various surface forces become operative when the film of liquid attains a thickness comparable to the particle diameter. These surface forces may induce film destabilisation and the formation of holes. Therefore, they have hypothesised that the particles rings in their experiments are formed as a result of the nucleation and expansion of holes in the wetting film at the final stage of its drying. The rim of the expanding hole drags the particles away and arranges them into annular rings as indicated in figure 13.

This theory can explain the holes formation but doesn't explain why there is a difference with increasing temperature of the substrate or why this phenomenon appears to occur more readily for low particle concentration.

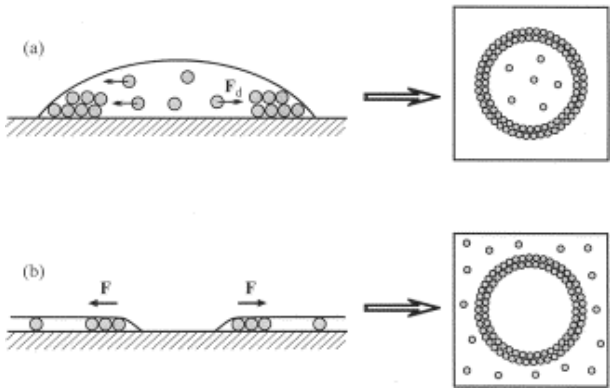

Fig. 13. two possible means of droplet evaporation with particles in suspension, (a) normal evaporation, (b) hole formation (Ohara, 1997)

Conclusion

Micro-PIV was used to study the evaporation of sessile droplets of water on both heated and non-heated glass substrates. Both the temperature of the glass substrate and the concentration of 1μm seeding particles in the water were varied. In all cases the dominant velocities along the base of the drop were found to be radially outwards from the centre of the drop. The velocity was found to increase with both temperature of the substrate and particle concentration in the water. The increase in velocity with particle concentration may be due both to deposited particles enhancing subsequent evaporation and to higher particle concentrations increasing the surface tension gradient along the air-water interface.

With higher particle concentration the thickness of the particle deposition at the contact line was found to increase: in all cases only limited deposition was found in the central region of the drop. This is consistent with the evaporation being dominant at the contact line.

Holes in the liquid film, and subsequent deposition pattern, were found to form in the latter stages of evaporation for heated substrates and low particle concentrations. The higher temperatures of the substrate probably lead to instability in thin liquid films evaporating, with localised thinning of the film leading to dry-out and depinning of the contact

line so-formed. Why this should be favoured at lower particle concentration is unclear, though it may be related to increases in surface tension at higher particle concentration.

References

Adachi, E., Dimitrov, A.S., Nagayama, K. 1995. Stripe patters formed on a glass surface during droplet evaporation. Langmuir 11, 1057−1060.

Anderson, D.M., Davis, S,H. 1995, The Spreading of volatile liquid droplets on Heated Surfaces, Phys Fluids, 7: 248−265.

Birdi, K.S., Vu, D.T., Winter, A. 1989, A study of the Evaporation Rates of small Water Drops placed on a Solid Surface, J Phys Chem, 93, 3702−3703.

Bourges-Monnier, C., Shanahan, M.E.R.1995, Influence of evaporation on contact angle, Langmuir, 11:2820−2829.

Deegan, R.D. 2000a. Pattern formation in drying drops. Phys. Rev. E 61, 475−485.

Deegan, R.D., Bakalin, O., Dupont, T.F., Huber, G., Nagel, S.R., Witten, T.A. 1997, Capillary flow as the cause of ring stains from dried liquid drops, Nature, 389, 827−829.

Deegan, R.D., Bakalin, O., Dupont, T.F., Huber, G., Nagel, S.R., Witten, T.A. 2000b, Contact Line deposits in an Evaporating Drop, Phys Rev E, 62, 756−765.

Fischer, B.J. 2002, Particle Convection in an Evaporating Colloidal Droplet, Langmuir, 18, 60−67.

Girard, F., Antoni, M., Sefiane, K. 2008. On the Effect of Marangoni Flow on Evaporation Rates of Heated Water Drops. Langmuir 24, 9207−9210.

Hu, H., Larson, RG.. 2002, Evaporating of a Sessile Droplet on a Substrate, J Phys. Chem. B 106, 1334−1344.

Hu, H., Larson, RG.. 2005a, Analysis of the Microfluid Flow in an Evaporating Sessile Droplet, Langmuir, 21, 3963−3971.

Hu, H., Larson, RG.. 2005b, Analysis of the effects of Marangoni Stresses on the Microflow in an Evaporating Sessile Droplet, Langmuir, 21, 3972−3980.

Hu, H., Larson, RG.. 2006, Marangoni Effect reverses Coffee-ring Depositions, J Phys. Chem. B, 110, 7090−7094.

Kang, K.H., Lee, S.J., Lee, C.M. 2003. Visualization of flow inside a small evaporating droplet. 5th International Symposium on Particle Image velocimetry, Busan, Korea Sept 22-24, paper 3242

Ohara, P.C., Gelbart, W.M. 1998, Interplay between hole instability and nanoparticle array formation in ultrathin liquid films, Langmuir, 14: 3418−3424.

Ristenpart, W.D., Kim, P.G., Domingues, C., Wan, J., Stone, H.A. 2007. Influence of substrate conductivity on circulation reversal in evaporating drops. Phys. Rev. Lett. 99, 234502.

Ruiz, O. E., Black, W. Z. 2002. Evaporation of Water droplets placed on a heated horizontal surface. J Heat transfer (Trans ASME) 124, 854−863.

Shmuylovich, L., Shen, A.Q., Stone, H.A. 2002. Surface morphology of drying latex fims: multiple ring formation. Langmuir 18, 3441−3445.

Uno, K., Hayashi, K., Hayashi, T., Ito, K., Kitano, H. 1998. Particle adsorption in evaporating droplets of polymer latex dispersions on hydrophilic and hydrophobic surfaces. Colloid Polym. Sci. 276, 810−815.

Van Nguyen, T. 2003. Influence of Surfactants on an evaporating drop: Fluorescence images and particle deposition patterns. Langmuir 12, 8271−8279

Xu, X., Luo, J. 2007. Marangoni Flow in an evaporating water droplet. Appl. Phys. Lett. 91, 124102

Zhang, N., Chao, D.F. 2001, Flow Visualization in Evaporating Liquid Drops and Measurement of Dynamic Contact Angles and Spreading Rate, J Flow Visualization and Image processing 8, 303−312.

Zhang, Y., Yang, S., Chen, L., Evans, J.R.G. 2008. Shape changes during the drying of droplets of suspensions. Langmuir 24, 3752−3758.